Many of the PHYS symposia are holding live Zoom sessions in addition to their ACS Broadcast and On-demand talks.

Connect via http://phys-acs.org/

or google PHYS ACS

(Speakers: please make this slide the first one in your on-demand ACS talk)

Computational Approaches for Li-O_2 Battery Design

Balachandran Radhakrishnan[1], Justin B. Haskins[2], John W. Lawson[2]

[1]KBR, Inc., NASA Ames Research Center
[2]NASA Ames Research Center

Green Aviation Battery Requirements

High Energy Density is a Major Requirement

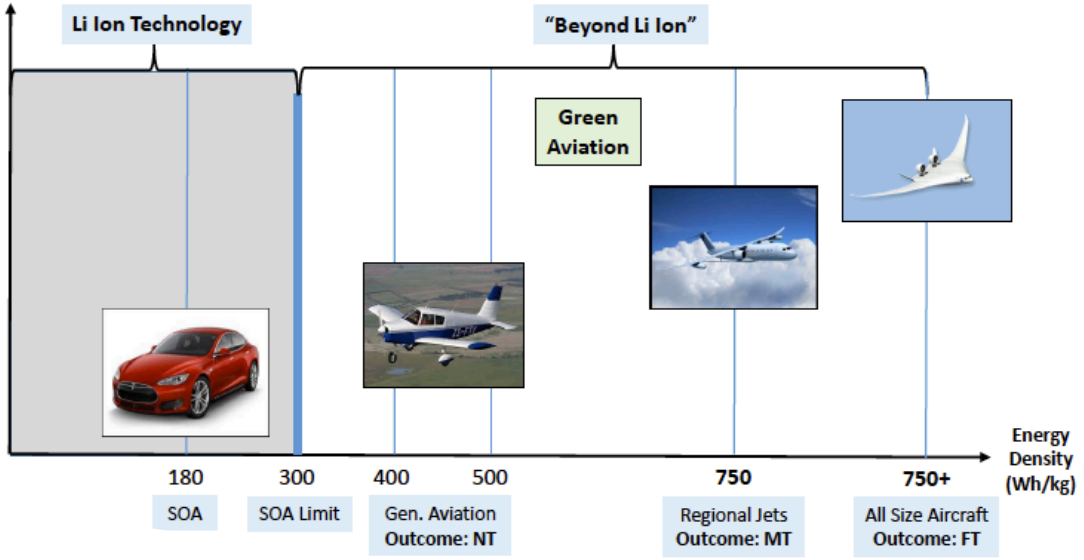

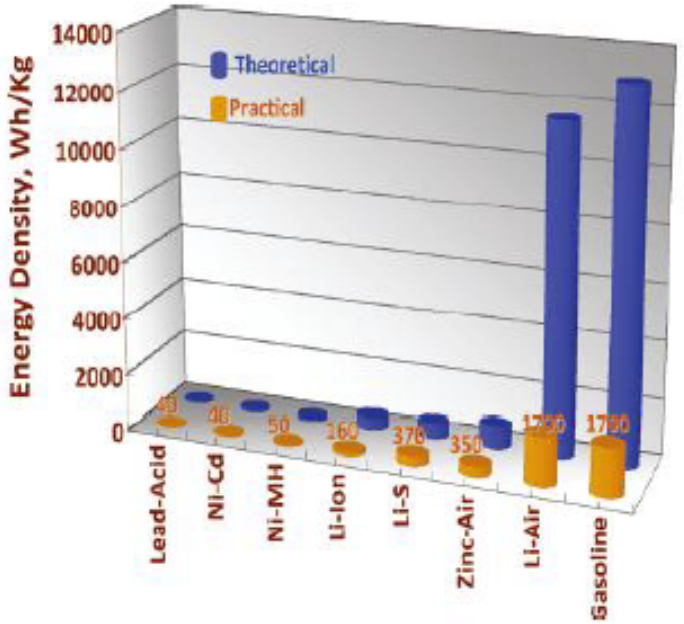

Li-O_2 batteries one means of realizing high energy density

Interfacial Studies in Li-O_2 batteries

- Li_2O_2 growth mechanism
  - Chemical disproportionation mechanism
  - Influence of solvent and surface charges
- Non-carbon cathode investigations
  - Carbon cathode decay
  - Non-reacting cathodes and surface reactions
- Molten Salt Electrolytes
  - High-temperature stable electrolyte
  - Effect of interfaces on electrochemical stability

Peroxide Growth - Toroids

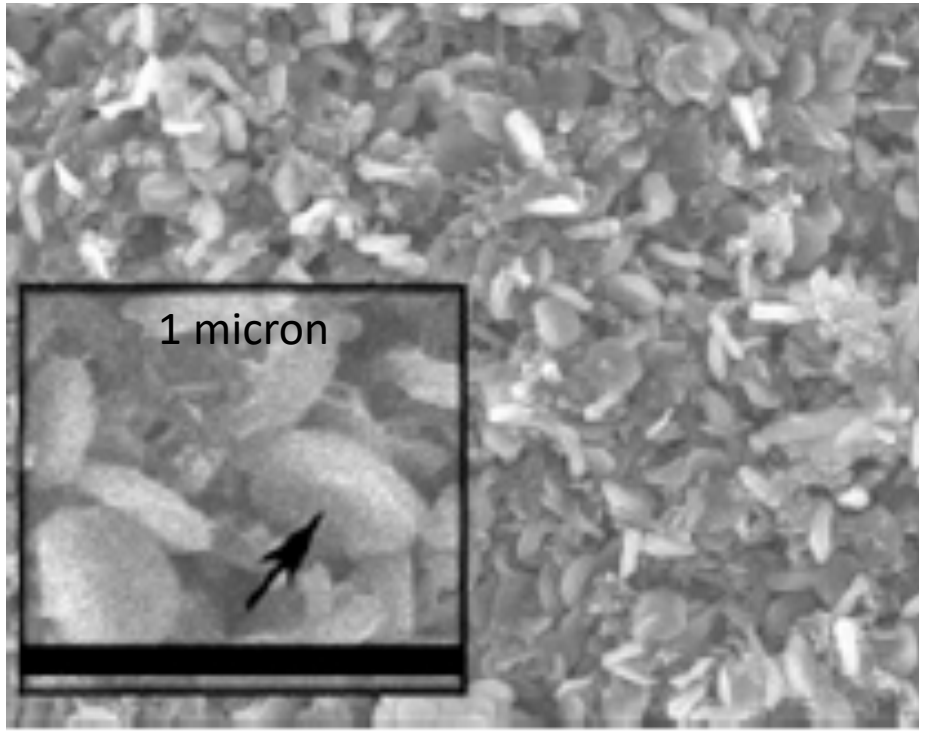

Chemical Disproportionation

$$(Li^+ + e^-) + O_2 \rightarrow LiO_2$$

$$2LiO_2 \rightarrow Li_2O_2 + O_2$$

Chemical disproportionation suggested as means to high-capacity toroidal growth of Li_2O_2
Disproportionation suggested to be highly dependent on surface potential and solvent effects

Burke, et al., PNAS (2015)

Previous Theoretical Investigations of Growth

DFT Simulations of Li Growth and Dissolution

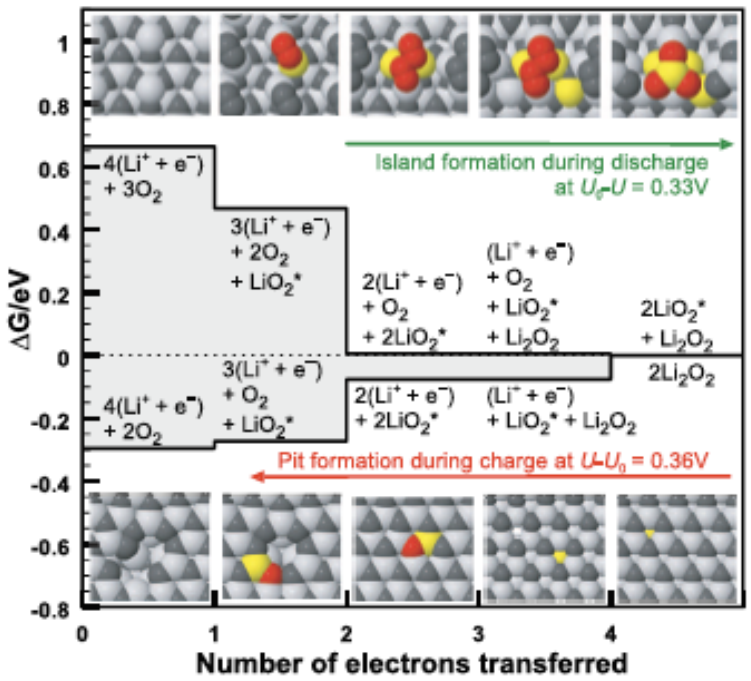

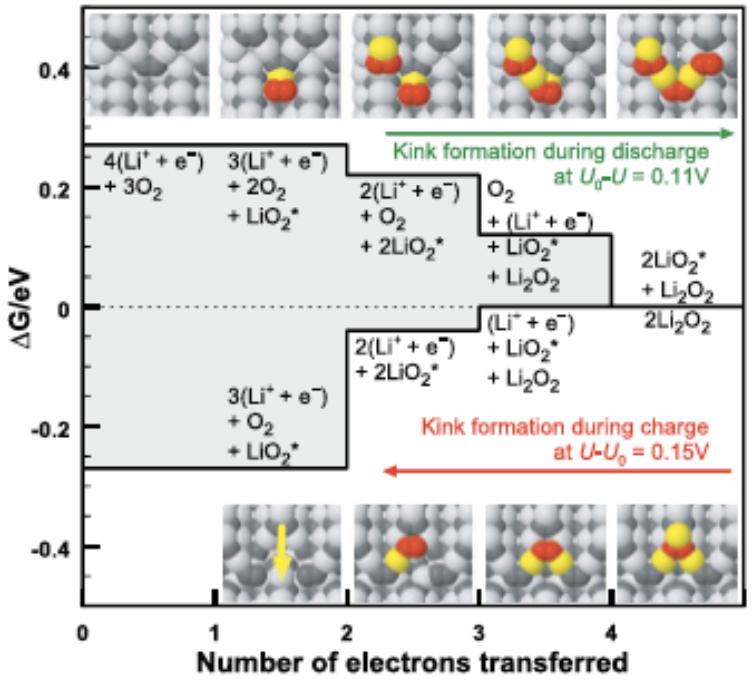

1) Previous work found low to moderate discharge overpotentials to growth
2) Approach not amenable to surface potential and solvation effects
3) Chemical disproportionation not yet addressed

Hummelshøj, et al., *J. Chem. Phys.* (2013)

Objectives

1) Formulate a new DFT model of electrochemical cell free energy that incorporates surface potential and solvation effects

2) Determine the influence of the new model on lithium peroxide growth overpotentials

3) Characterize chemical disproportionation with the new model

Constant Potential and Solvation

Charged Surface

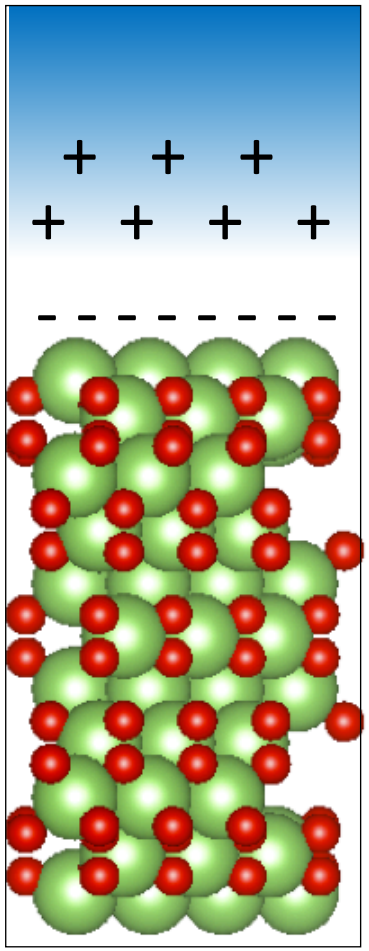

Goodpaster, et al., *J Phys. Chem. C* (2016)

Charge is added until a target *U* is met

$$U = \frac{-\epsilon_F - \phi_{SHE}}{e}$$

Surface charge is screened using JDFT *via* VASPsol (linearized Poisson-Boltmann)

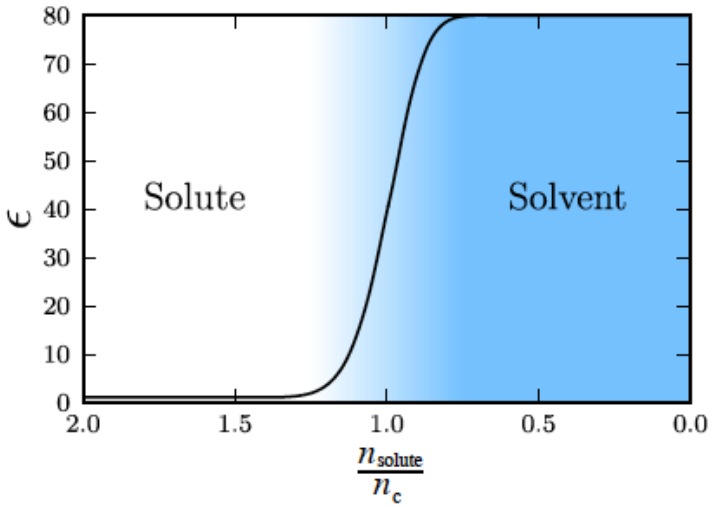

Mathew, et al., *J. Chem. Phys.* (2014)

Model Calibration to Dimethoxyethane (DME)

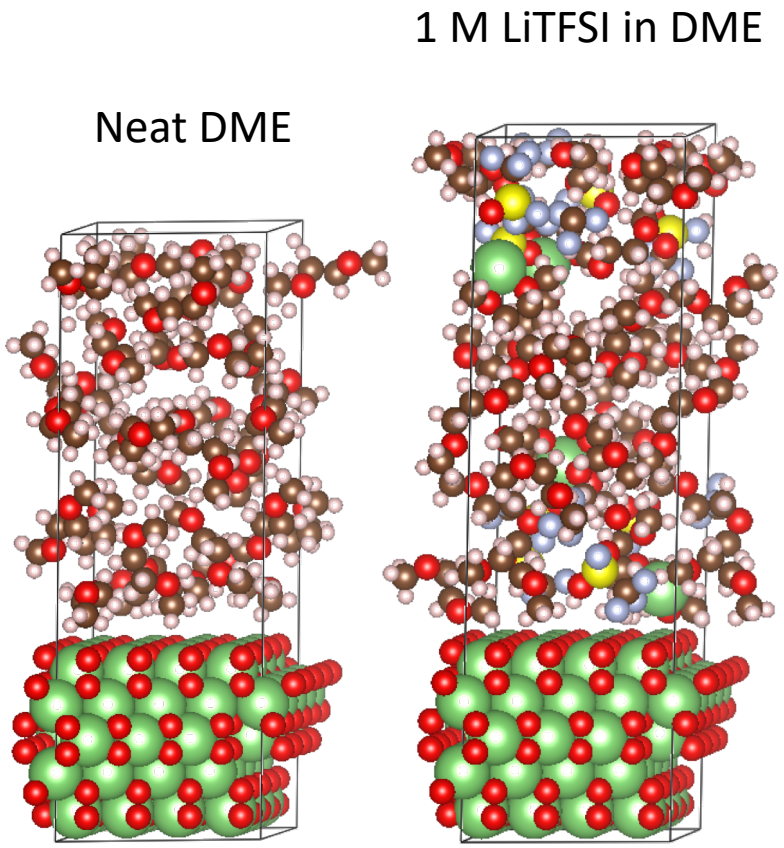

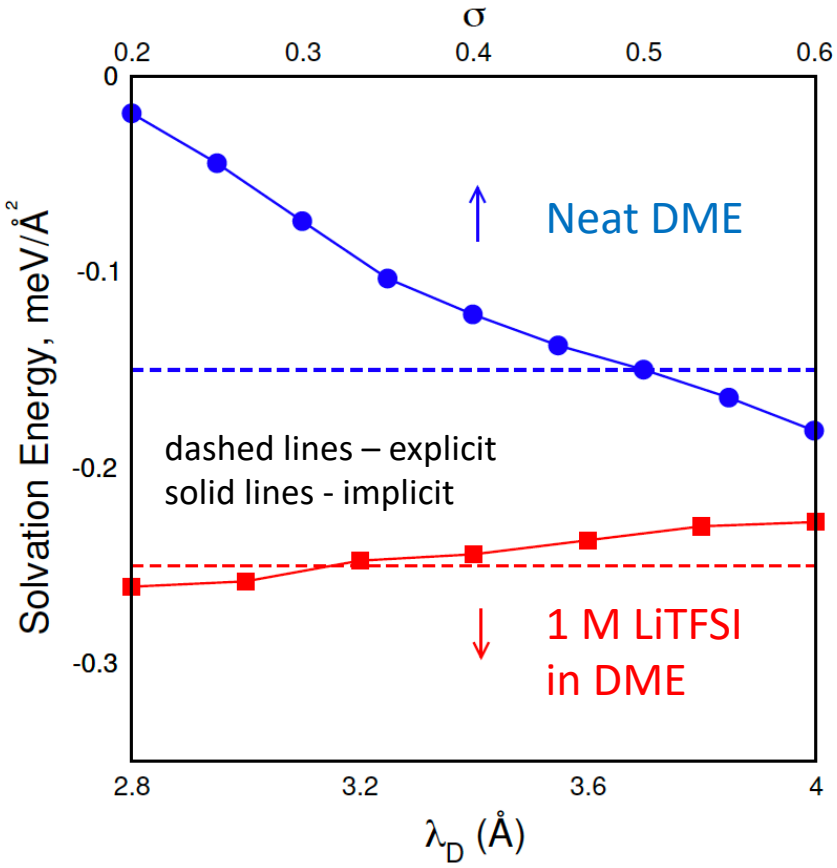

Implicit solvent can reproduce explicit DME solvation

1) Interface Model

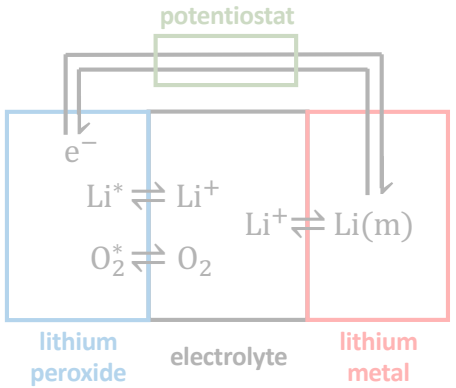

2) Growth Overpotentials

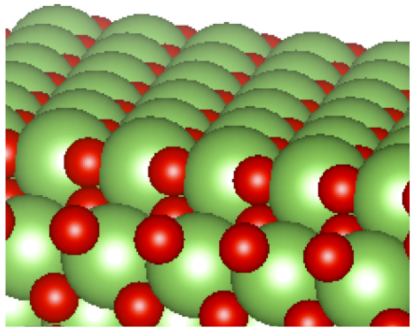

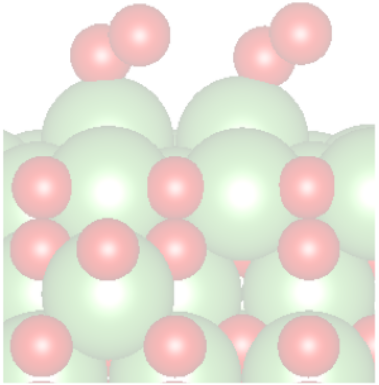

3) Chemical Disproportionation

Surface Free Energies

Previous Model

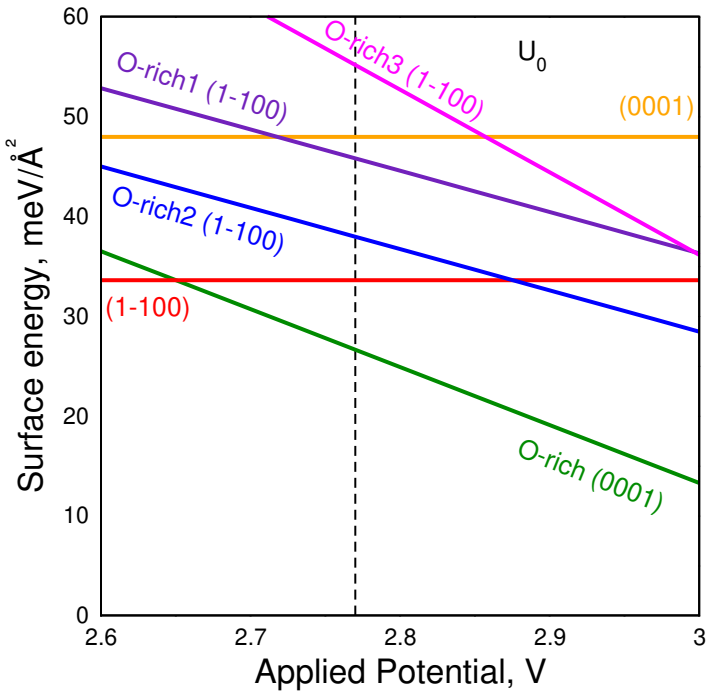

New Model

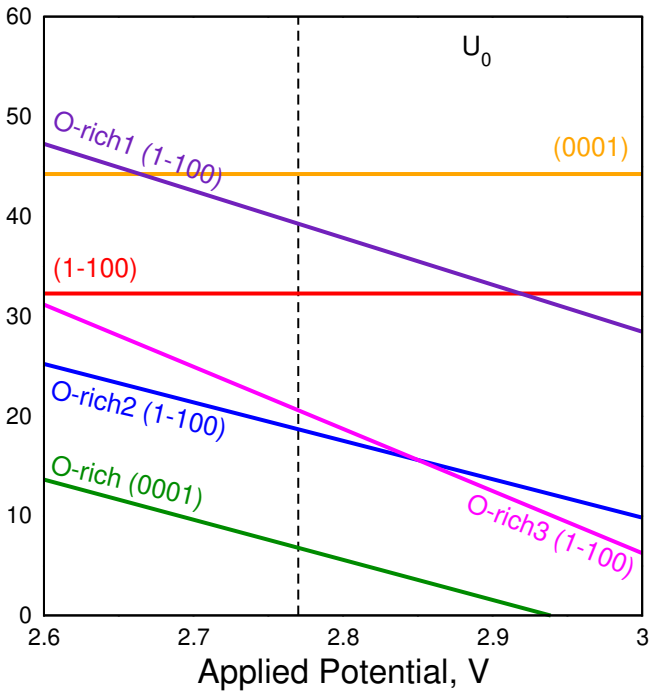

Increasing potential leads to more favorable Li_2O_2 growth, surface charge and solvation decrease surface free energy

Surface Free Energies

O-rich (0001)

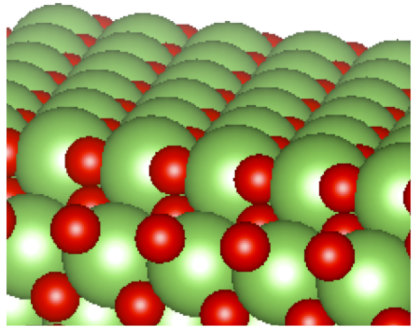

O-rich2 (1-100)

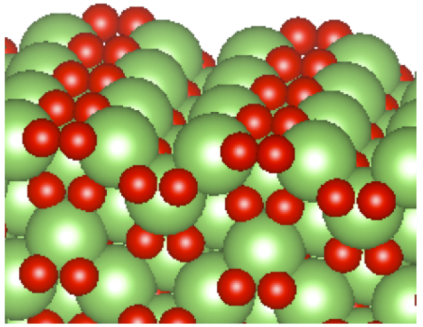

New Model

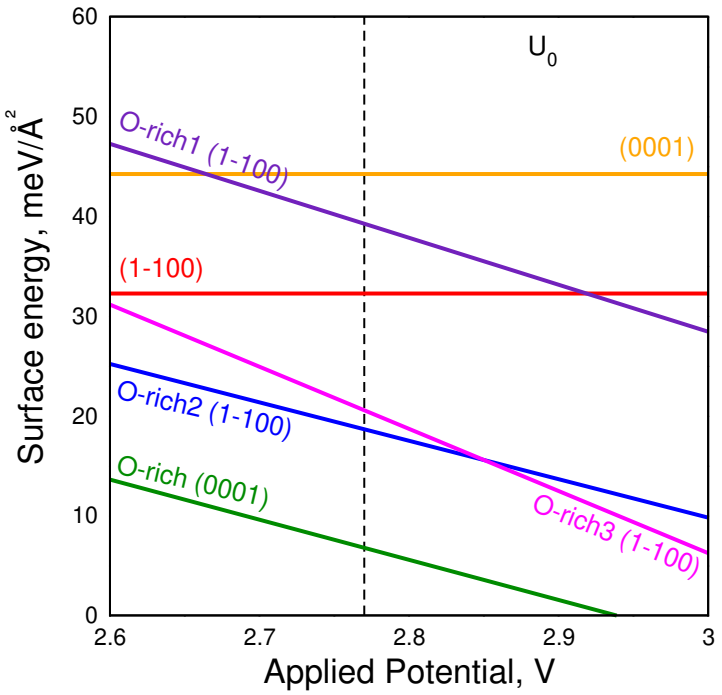

(0001) and (1-100) surfaces are most stable near discharge potentials

Growth and Overpotentials on (0001)

Island Growth Path on O-rich (0001)

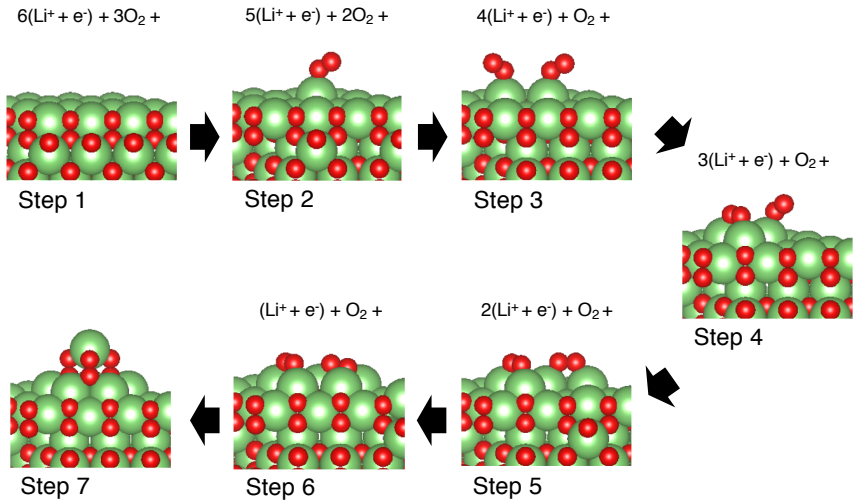

Overpotentials

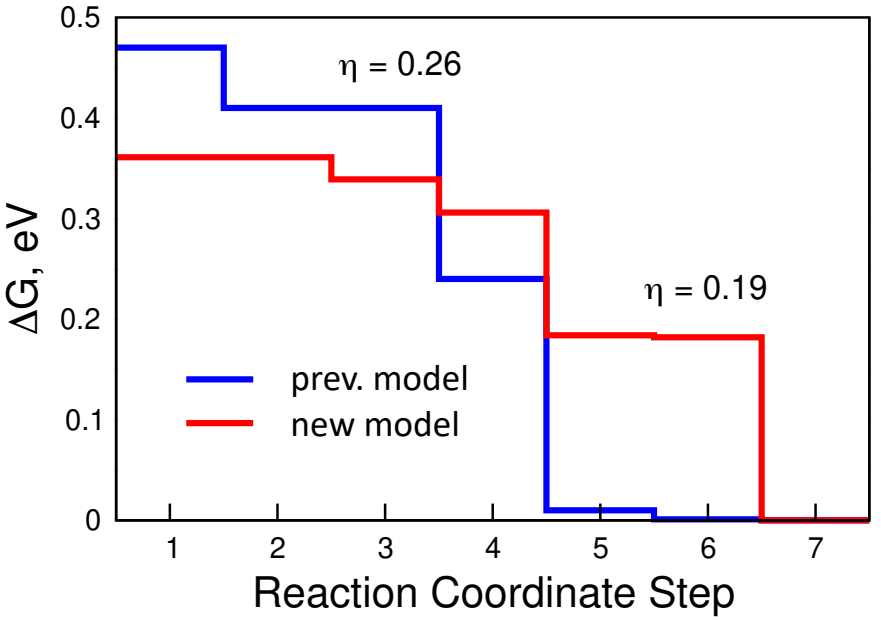

Limiting step is addition of first or second LiO_2
Solvation and surface charge decrease (0001) overpotentials

Path similar to that from Hummelshøj, et al., *J. Chem. Phys.* (2013)

Growth and Overpotentials on (1-100)

Island Growth Path on O-rich2 (1-100)

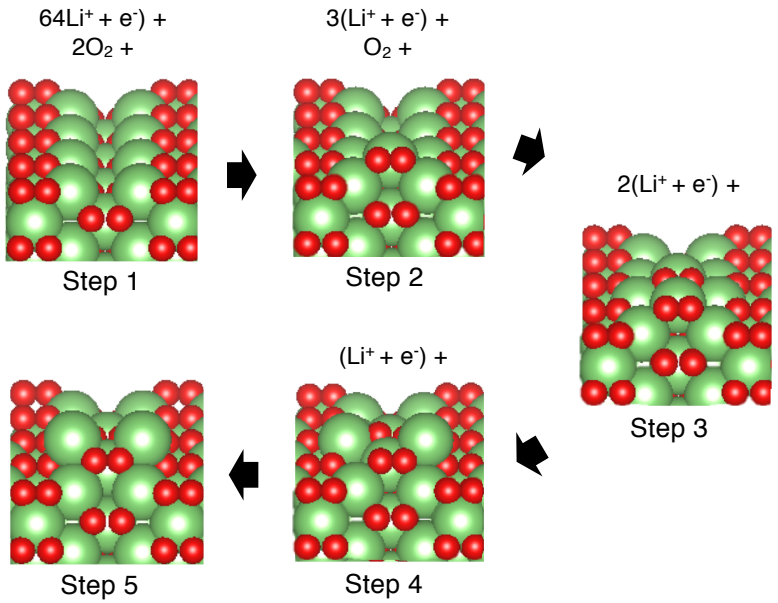

Overpotentials

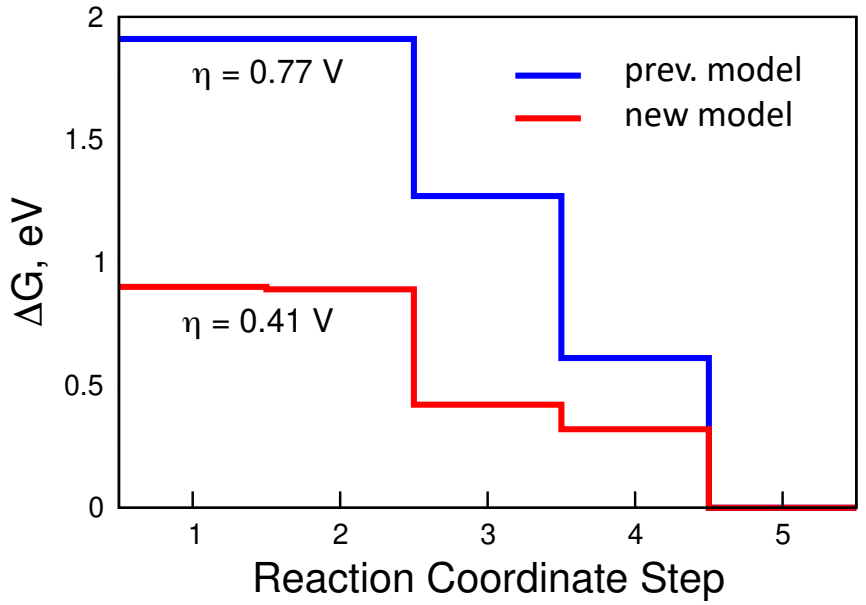

Limiting step is addition of first LiO_2
Solvation and surface charge decrease (1-100) overpotentials

Path similar to that from Hummelshøj, et al., *J. Chem. Phys.* (2013)

1) Interface Model

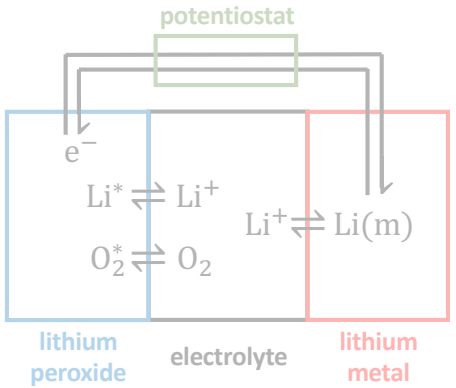

2) Growth Overpotentials

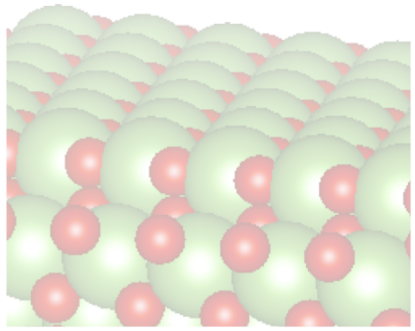

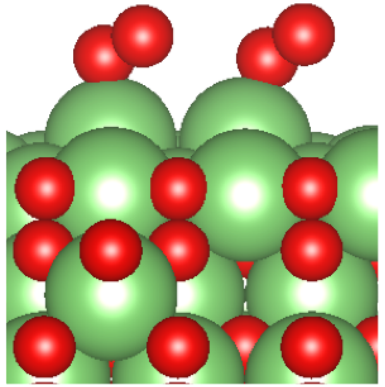

3) Chemical Disproportionation

Chemical Disproportionation Kinetics

(0001) Disproportionation

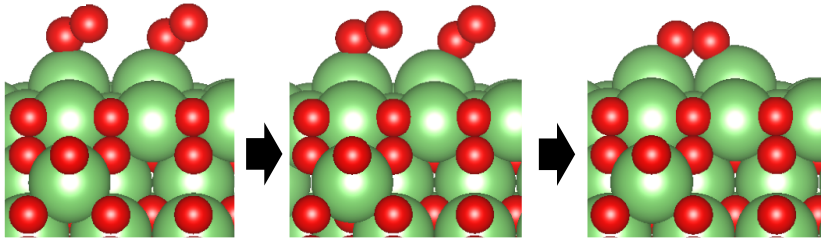

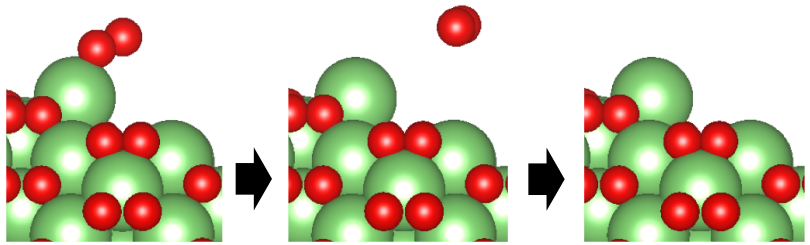

(1-100) Disproportionation

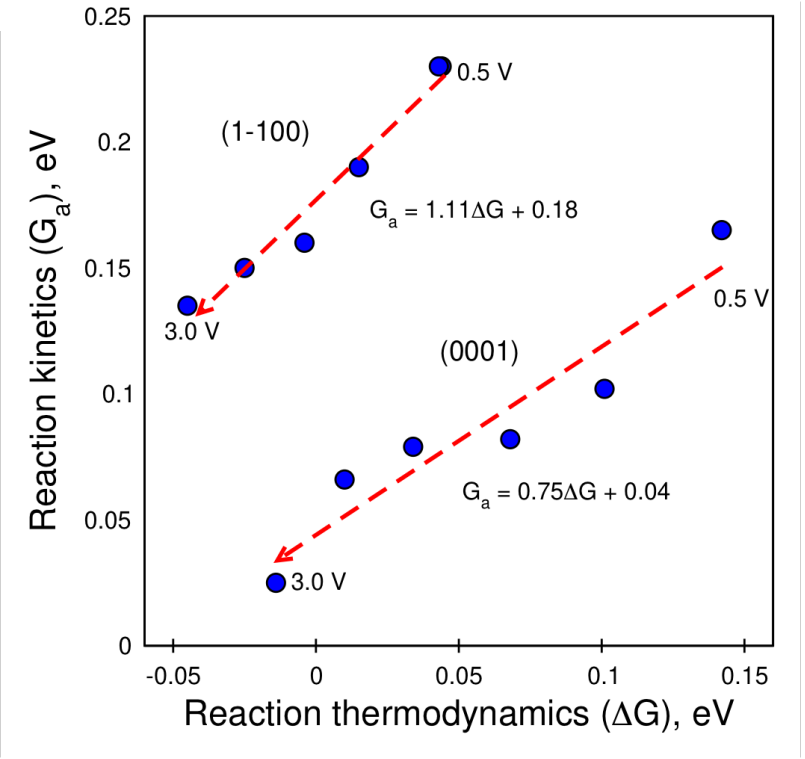

Small barriers to disproportionation - smaller on (0001) surface
Favorable energetics at discharge potentials
Exhibits Bell-Evans-Polanyi principle (linear relationship)

Conclusions

- Cell free energy model developed that incorporates effects of solvation and surface charge
- Poisson-Boltzmann formalism calibrated to DME and used to perform constant potential density functional theory calculations
- Influence of solvation and potential is to lower surface free energies and overpotentials
- Chemical disproportionation is found to be a viable growth mechanism with low barriers
- Kinetics and thermodynamics of disproportionation imply a relationship akin to Bell-Evans-Polanyi

Non-carbon cathodes: Motivation

- Li-O_2 electrochemistry

$$Li^+ + O_2(g) + 2e^- \leftrightarrow Li_2O_2^*$$

- Parasitic reactions with electrode and electrolyte lead to capacity loss and abysmal cycles
- Carbon cathodes decay over the charge-recharge cycle

$$Li_2O_2 + \frac{1}{2}O_2 + C \leftrightarrow Li_2CO_3^*$$

- Possible solution: Search for non-carbon cathodes with desired properties

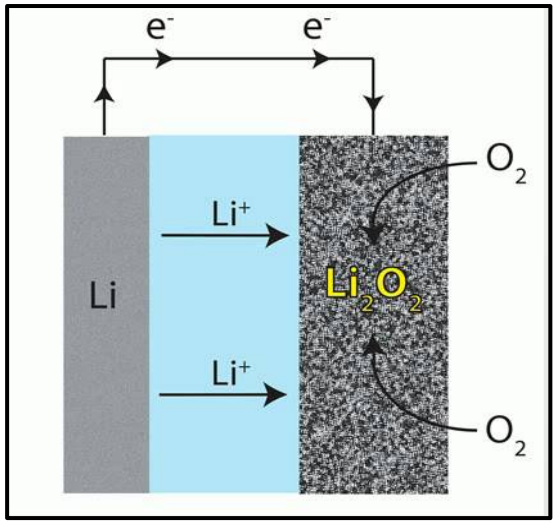

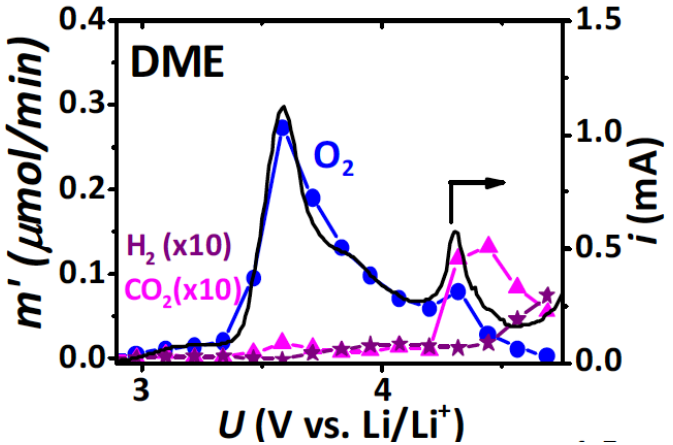

J. Phys. Chem. Lett. 2012, 3, 3043−3047

Non-carbon ideal electrode

Preferred properties of cathode in Li-O_2 battery:

1. Stability against Li_2O_2, the deposition product
2. No side reactions with electrolytes and intermediates in the electrochemistry
3. Electrochemical stability in the operating voltage range
4. Promoting formation of Li_2O_2

Transparent Conducting Oxides as cathodes

1. Stable in ether type electrolytes (DME, TEGDME etc)
2. Band gap controlled and commercially available
3. Stable in oxygen rich environment
4. Can they satisfy requirements of cathode in Li-O_2 battery?

Chemical Stability: Phase Diagrams

Phase Diagram constructed using DFT energies from [1]Materials Project

Any chemistry that has a non-intersecting tie-line with Li_2O_2 is stable against it

Intersecting tie-line gives the reaction products with Li_2O_2

ZnO, In_2O_3 and CdO are stable against Li_2O_2

SnO_2 reacts with Li_2O_2 to form Li_2SnO_3

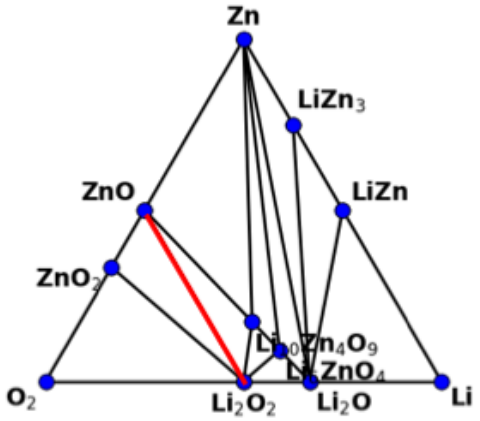

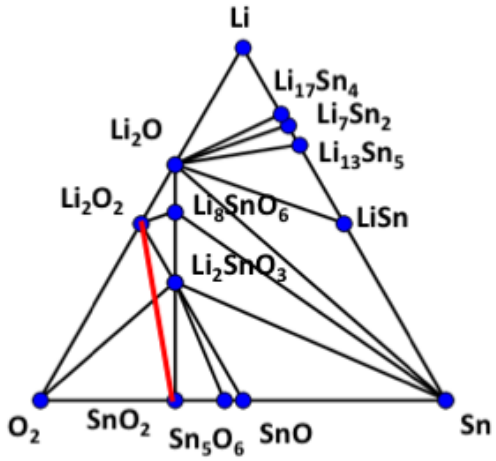

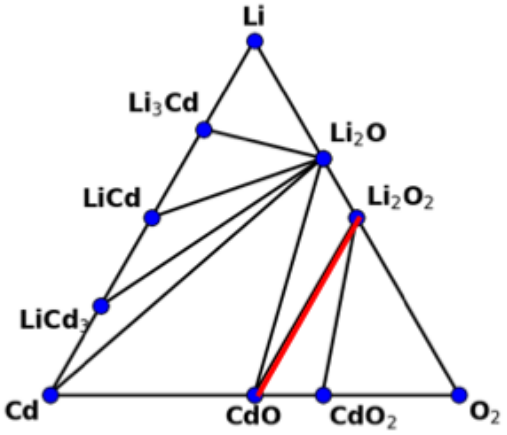

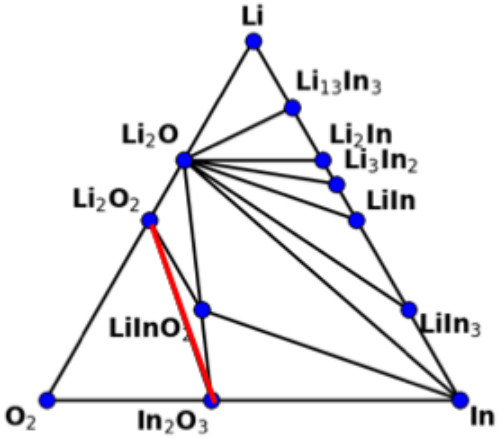

$$\Delta E(\in, Li_2O_2) = \min_{0 \le x \le 1} E_{x.\in-(1-x).Li_2O_2} - x.E_{\in} - (1-x).E_{Li_2O_2}$$

1. Comp. Mater. Sci., 68, 314–319 (2013)

Ref: J. Phys. Chem. C 2019, 123, 8, 4623-4631

Electrochemical stability

Grand potential phase diagram is constructed to predict electrochemical stability range of the electrode

$$\emptyset = E - \mu_{Li} N_{Li}$$

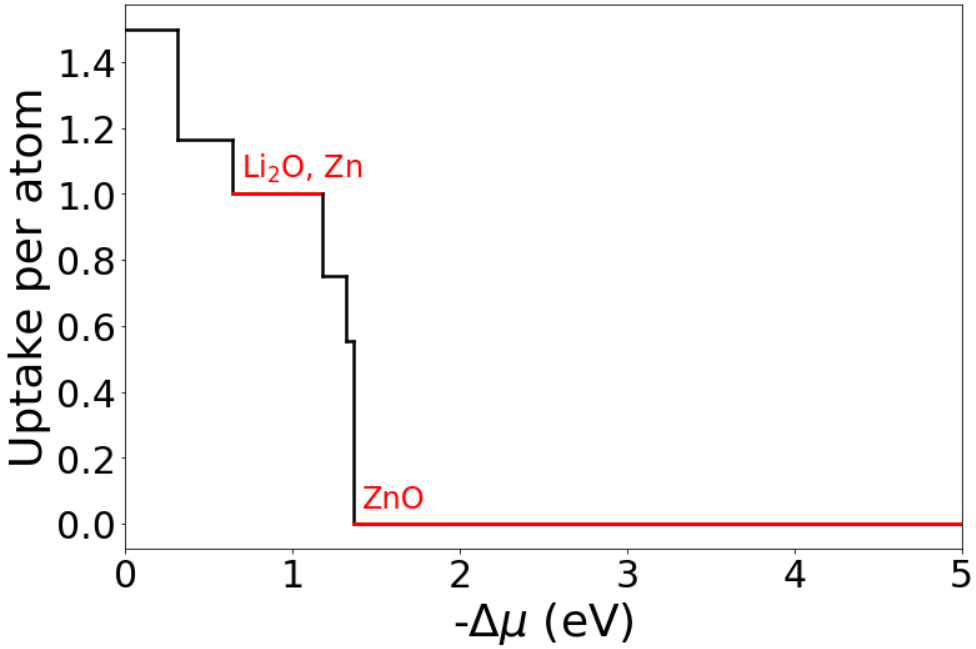

Cathode	Electrochemical stability (V) (vs Li)
SnO_2	>1.98
CdO	>1.72
In_2O_3	>1.58
ZnO	> 1.36

All the TCOs considered in this study are stable in the operating voltage of 2-4.5 V

APL Materials 1 , 011002 (2013); Comp. Mater. Sci., 68, 314–319 (2013)

Ref: J. Phys. Chem. C 2019, 123, 8, 4623-4631

Surface of interest

- Identify surfaces of interest using Wulff shape construction
- Surface energy is a function of chemical potential of oxygen
- Oxygen rich and oxygen deficient environments produce different crystal shapes
- ZnO can be synthesized as thin film (0001) as well as needle structures $(10\bar{1}0)$

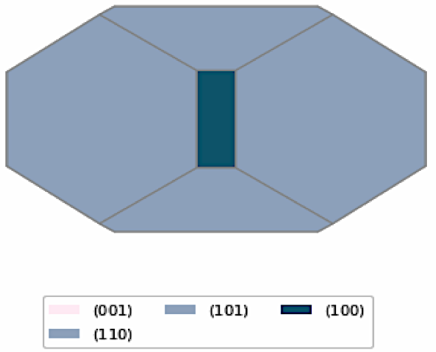

SnO_2

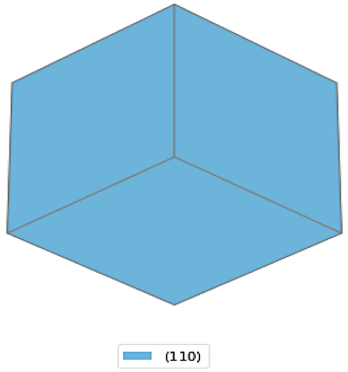

CdO

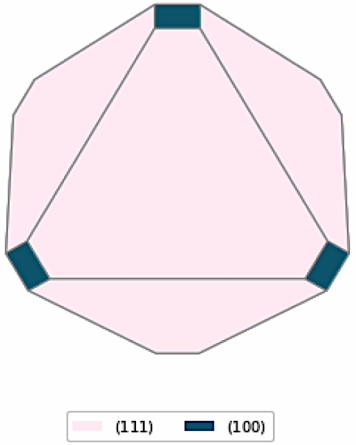

In_2O_3

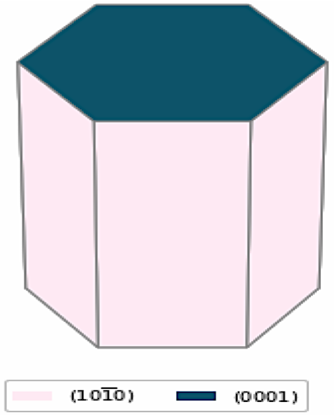

ZnO

$$\gamma_{surf} = \frac{1}{2A}\left[E_{slab}(N_M N_O) - \frac{N_M}{x}E_{bulk}(M_x O_y) + \left(\frac{N_M}{x}y - N_O\right)\mu_O\right]$$

Adsorption Studies

Li_2O_2: 2 electron process:

a. $Li^+(solv) + O_2(g) + e^- \leftrightarrow LiO_2^*$

b. $Li^+(solv) + LiO_2^* + e^- \leftrightarrow Li_2O_2(s)$

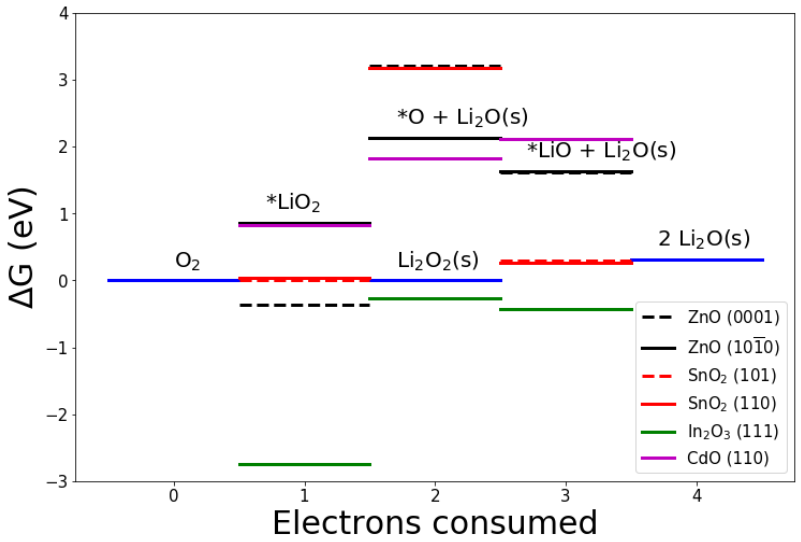

Li_2O: 4 electron process

a. $Li^+(solv) + O_2(g) + e^- \leftrightarrow LiO_2^*$

b. $Li^+(solv) + LiO_2^* + e^- \leftrightarrow Li_2O(s) + O^*$

c. $Li^+(solv) + Li_2O(s) + O^* + e^- \leftrightarrow LiO^* + Li_2O(s)$

d. $Li^+(solv) + LiO^* + Li_2O(s) + e^- \leftrightarrow 2Li_2O(s)$

- ZnO (0001) most suitable for Li_2O_2 formation
- SnO_2 will lead to mix of Li_2O and Li_2O_2 formation
- In_2O_3 and CdO promote Li_2O formation

ACS Energy Lett., 1, 162−168 (2016)

Ref: J. Phys. Chem. C 2019, 123, 8, 4623-4631

Doping TCOs

- TCOs are small band-gap materials in pristine condition
- Vacancy induced electronic conductivity observed
- Considered %~2 at. wt. doping in ZnO
- Used thermodynamic energetics to determine interstitial vs substitutive doping

Substitutional dopant $48\ ZnO + X \rightarrow Zn_{47}XO_{48} + Zn$		Interstitial dopant $48\ ZnO + X \rightarrow Zn_{48}XO_{48}$	
Doped Chemistry	Dopant Formation Energy (eV)	Doped Chemistry	Dopant Formation Energy (eV)
$Zn_{47}AlO_{48}$	-1.75	$Zn_{48}AlO_{48}$	2.153
$Zn_{47}GaO_{48}$	0.83	$Zn_{48}GaO_{48}$	4.417
$Zn_{47}GeO_{48}$	2.56	$Zn_{48}GeO_{48}$	5.502
$Zn_{47}InO_{48}$	1.97	$Zn_{48}InO_{48}$	5.182
$Zn_{47}SiO_{48}$	-1.608	$Zn_{48}SiO_{48}$	2.536
$Zn_{47}SnO_{48}$	4.15	$Zn_{48}SnO_{48}$	7.52

Al, Si and Ga substitutional doping was considered for further studies

Ref: J. Phys. Chem. C 2019, 123, 8, 4623-4631

Effect of Doping

Boltzmann semi-classical equations

$$\sigma_{\alpha\beta\gamma}(i,k) = e^3 . \tau^3_{(i,k)} . \varepsilon_{\gamma uv} . v_{\alpha(i,k)} v_v(i,k) M^{-1}_{\beta u}$$

$$M^{-1}_{\beta u}(i,k) = \frac{1}{\hbar^2} \frac{\partial^2 \varepsilon_(i,k)}{\partial k_\beta \partial k_u}$$

DFT computations using HSE06 hybrid functional

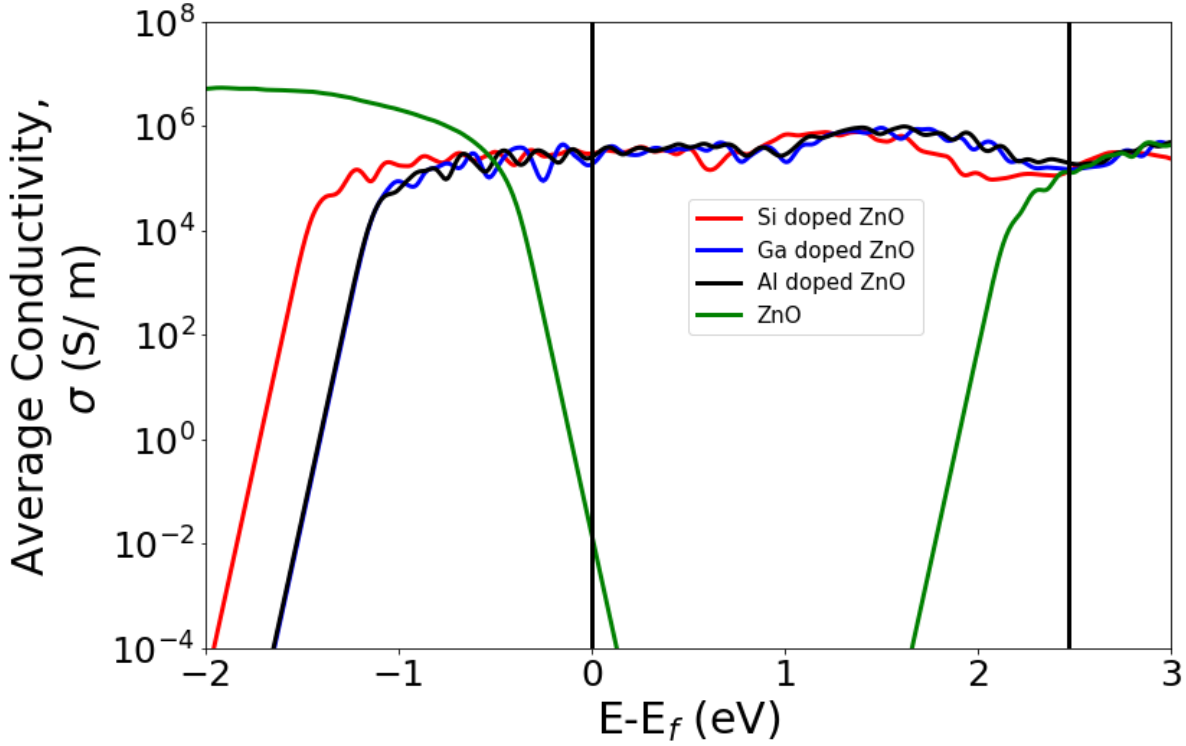

BoltzTraP: Computer Physics Communications 2006, 175, 67-71

Ref: J. Phys. Chem. C 2019, 123, 8, 4623-4631

Effect of doping

Doped (0001) ZnO

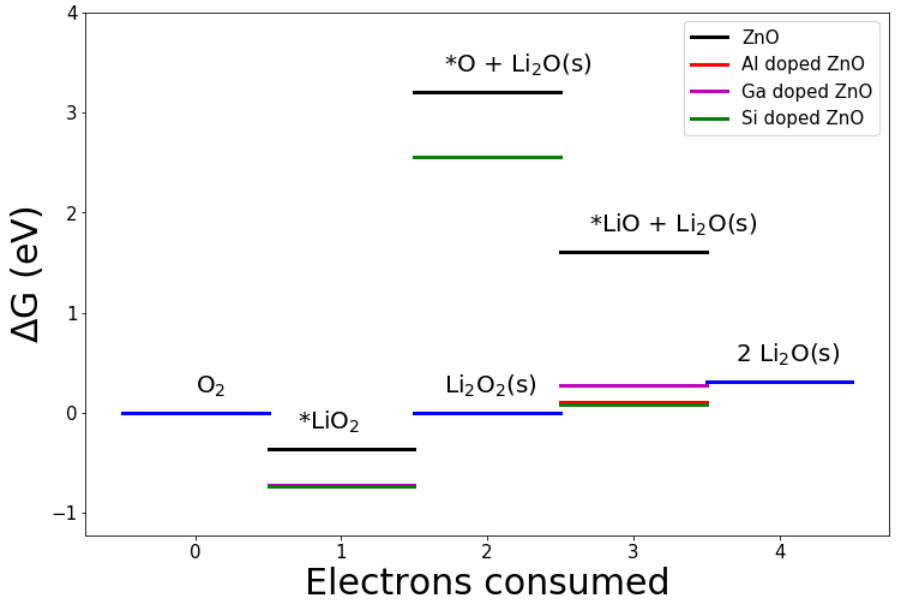

Doped (10$\bar{1}$0) ZnO

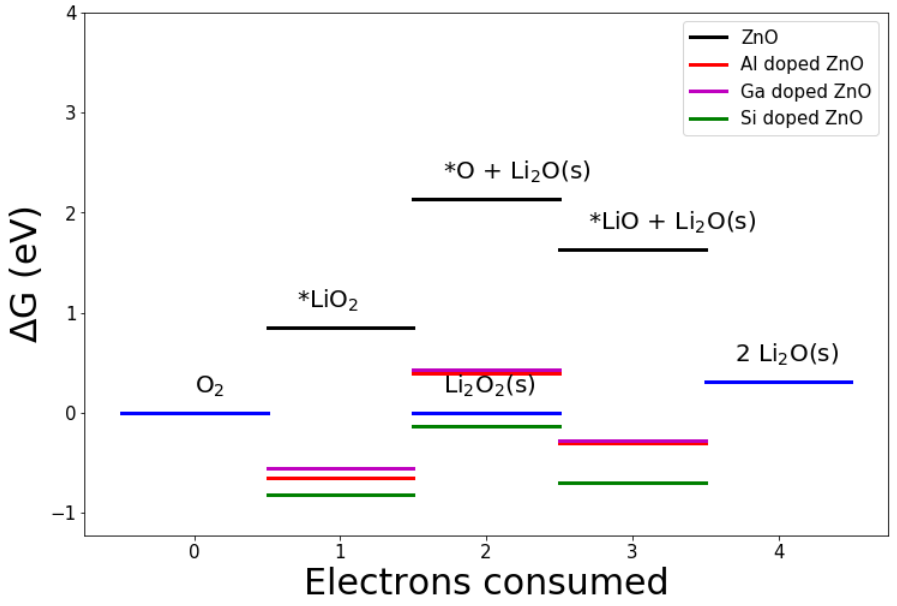

- Doping leads to better adsorption of LiO_2^* intermediate
- (10$\bar{1}$0) surface, on doping, promotes formation of Li_2O
- Doped (0001) surface binds LiO_2^* favorably while maintaining a viable path to Li_2O_2 formation

Ref: J. Phys. Chem. C 2019, 123, 8, 4623-4631

Other oxides…

Only those oxides that are chemically stable against Li_2O_2 were considered

Chemistry	Electrochemical stability range (V) (vs Li/Li^+)	Notes
BeO	≥ 0	Toxic
MgO	≥ 0.64	Insulator
K_2O_2	≥ 2.4	Prone to Li^+attack
CaO	≥ 0	Promising candidate with doping
SrO_2	≥ 2.89	Prone to Li^+attack
BaO_2	≥ 2.68	Prone to Li^+attack
CsO_2	≥ 2.88	Conductor
Y_2O_3	≥ 0	Promising candidate with doping
La_2O_3	≥ 0	Promising candidate with doping
CeO_2	≥ 1.22	Used as coating[42]
Sm_2O_3	≥ 0	Rare earth mineral
Gd_2O_3	≥ 0	Rare earth mineral
Tb_2O_3	≥ 0	Rare earth mineral
Dy_2O_3	≥ 0	Rare earth mineral
Er_2O_3	≥ 0	Rare earth mineral
Tm_2O_3	≥ 0	Rare earth mineral
Lu_2O_3	≥ 0	Rare earth mineral
HgO	2.45	Toxic

Ref: J. Phys. Chem. C 2019, 123, 8, 4623-4631

Molten Salt Electrolytes

- Molten salt electrolytes:
  - $LiNO_3$ + KNO_3 eutectic
  - Melting point: 125 ^oC
  - Operating temperature: 150 ^oC
  - Other known mixtures: $LiNO_3$+ $CsNO_3$+ KNO
  - No known decomposition of the electrolyte
  - Cycles limited by decomposition of carbon-cathode

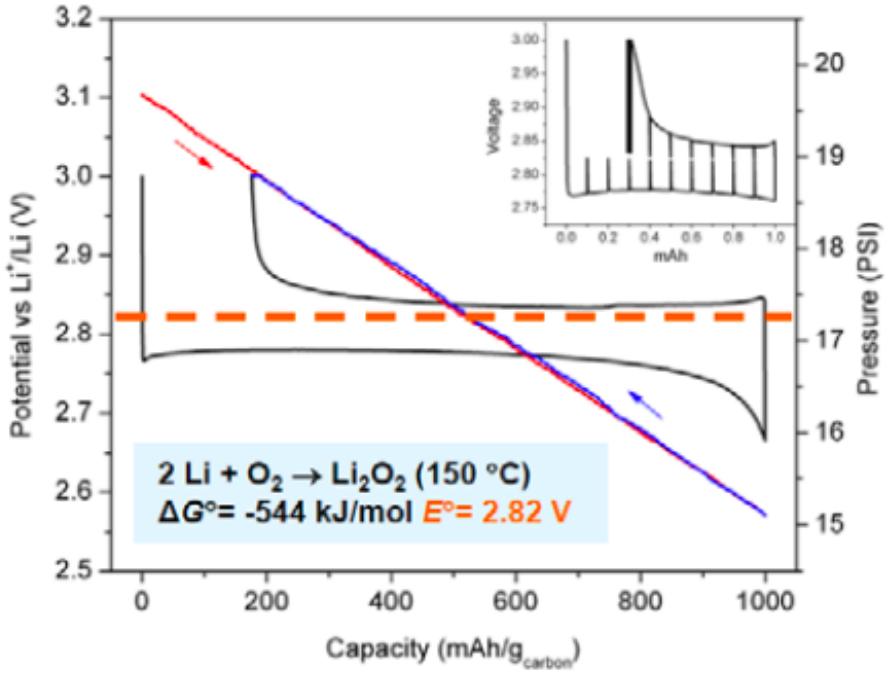

Ref: LiOX Power Inc

Transport properties

- AIMD simulations were performed on the eutectic mixture
  - 100 ps simulations
  - Simulations at 523 K to 673 K in steps of 50 K

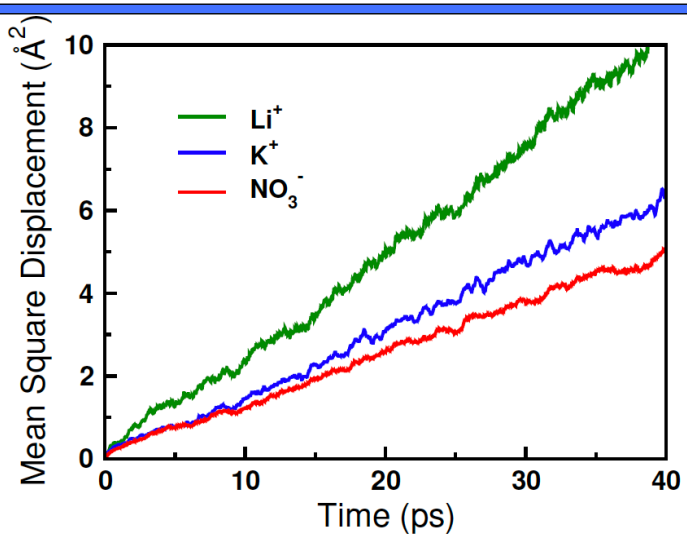

MSD @ 673 K

- Computed ionic conductivity matches well with experiments
- Correlations are more pronounced due to cell-size effects

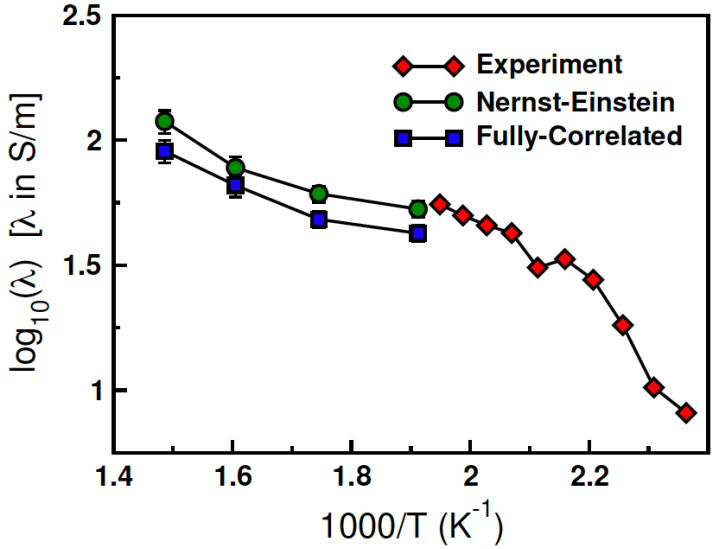

Transport properties

- Li^+ more closely coordinated by anions compared to K^+
- Coordination of NO3-ions appear bimodal based on the pronounced shoulder in the radial distribution function
- Transference number (t^{Li+}) is ~0.35 while experiments report ~0.6 as they do not account for t^{K+}

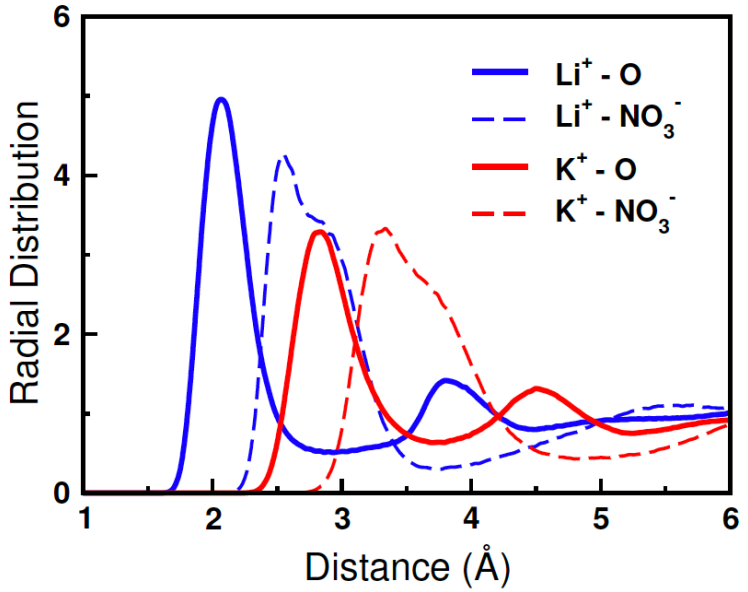

Ratio of correlated to uncorrelated ionic conductivity (α), transference number(t^{Li+}), and ionic conductivity attributed to Li+ (λ^{Li+}).

T	α	t^{Li+}	λ^{Li+}
523	0.80	0.35	14.6
573	0.79	0.30	14.7
623	0.85	0.34	22.3
673	0.76	0.31	27.6

Electrochemical properties

- Grand potential analysis and band structure computations point towards larger electrochemical windows
- Experiments show a narrower electrochemical window: 2.1 V -3.6 V (vs Li/Li^+)

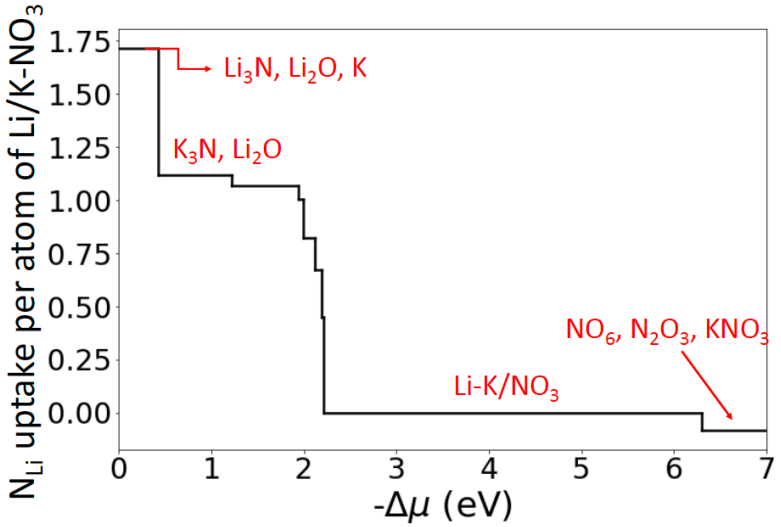

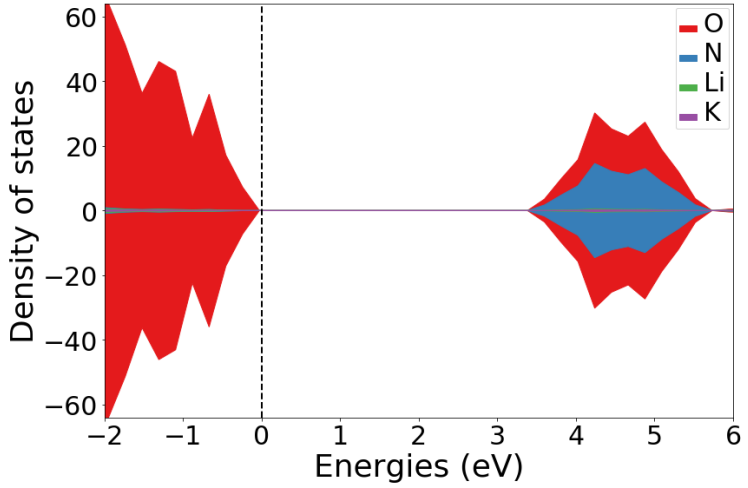

Electrochemical properties

- Grand potential analysis and band structure computations point towards larger electrochemical windows
- Experiments show a narrower electrochemical window: 2.1 V -3.6 V (vs Li/Li^+)
- Interfacial reactions predict formation of K_2CO_3
- K_2CO_3 decomposes at 3.6 V (vs K/K^+)
- Interfacial reactions determine electrochemical stability of the nitrates
- Catalysts can alter these stability windows as well[1]

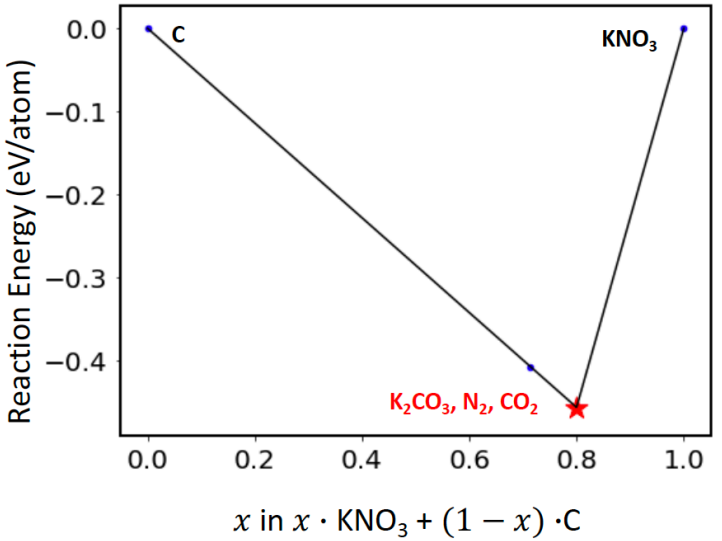

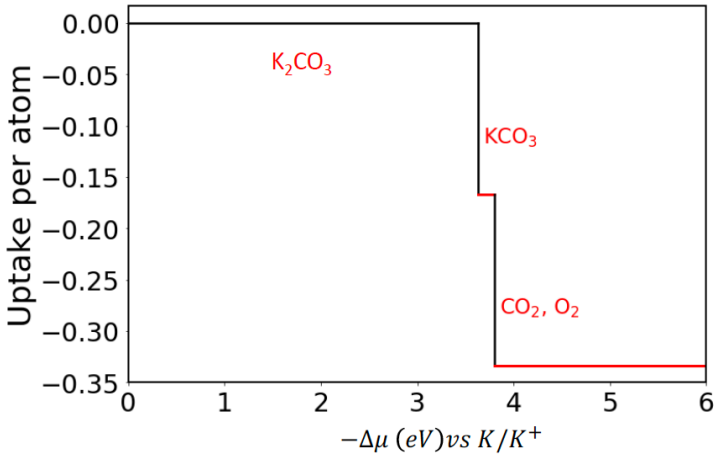

1. Giordani, V.; et. al, Nature chemistry 2019, 11, 1133-1138.

Summary

- Interfacial phenomena are critical to realizing a stable Li-O_2 electrochemistry
- Li_2O_2 deposition mechanism influenced by surface charges as well as solvent
- Non-carbon cathodes: Stable cathodes that promote formation of Li_2O_2
- Nitrate electrolytes: Neither solid nor organic liquids, but can provide best of both worlds in ionic-transport and wettability
- Nitrates: Interfacial reactions determine electrochemical properties

Acknowledgements

NASA Convergent Aeronautics Solutions (CAS) Project Collaborators

NASA

Charles Bauschlicher

Balachandran G Radhakrishnan

Mohit Mehta

Donald Dornbusch

Fred Dynys

William Bennett

James Wu

Vadim Lvovich

UC Berkeley

Kristian Knudsen

Bryan McCloskey